The Molecular Structure of Molybdenum Pentachloride Studied by *Ab Initio* Molecular Orbital Calculations and Gas Electron Diffraction

Knut Fægri, Kjell-Gunnar Martinsen, Tor G. Strand* and Hans Vidar Volden

Department of Chemistry, University of Oslo, Box 1033 Blindern, N-0315 Oslo, Norway

Fægri, K., Martinsen, K.-G., Strand, T. G. and Volden, H. V., 1993. The Molecular Structure of Molybdenum Pentachloride Studied by *Ab Initio* Molecular Orbital Calculations and Gas Electron Diffraction. – Acta Chem. Scand. 47: 547–553.

Molecular orbital calculations for highly symmetric conformers of gas-phase $MoCl_5$ at three levels [all-electron restricted Hartree–Fock (RHF) calculations, relativistic effective core potential (RECP) RHF calculations and modified coupled pair functional RECP calculations] have been carried out. The calculations indicate that a D_{3h} structure is more stable than a C_{4v} configuration by 10–11 kcal mol^{-1}. A distortion from D_{3h} to C_{2v} symmetry splits the orbitally degenerate $^2E''$ electronic state into $^2B_1$ and $^2A_2$ states, which are stabilized by 0.24 and 0.35 kcal mol^{-1}, respectively, at the RECP RHF level, suggesting that the molecule may undergo a dynamic Jahn–Teller distortion. Gas electron-diffraction data of $MoCl_5$ were best fitted by distorted trigonal bipyramidal models of C_{2v} symmetry with large-amplitude motion. A simple dynamical model for the electron-diffraction data based on the *ab initio* results allowed the refinement of three structural parameters to yield good agreement with the electron-diffraction data. The results of the two methods agree if a relatively flat potential for the distortion towards the C_{4v} form is assumed. Electron diffraction as well as *ab initio* calculations exclude a possible pseudorotation by the Berry mechanism over a C_{4v} barrier.

While solid molybdenum pentachloride is known to be dimeric with distorted octahedrally coordinated Mo atoms joined by two Cl bridges,[1] several studies have been carried out to establish the shape of the gaseous monomer.[2] Two previous investigations by gas electron diffraction (GED) yielded trigonal bipyramidal D_{3h} structures.[3,4] A third GED study found that neither a trigonal bipyramidal nor a square pyramidal C_{4v} model agreed satisfactorily with the data, but that agreement could be obtained for a mixture of molecules with D_{3h} and C_{4v} symmetries, and a small amount of metal–metal bonded dimers.[5] The gas-phase Raman spectrum of the molecule has been found to be consistent with a trigonal bipyramidal structure,[6] while the IR spectrum of the matrix isolated species has been assigned on the basis of C_{4v} symmetry.[7]

Recently, a GED investigation showed that the coordination geometry of hexamethyltungsten was trigonal prismatic rather than octahedral.[8] In view of this result, monocapped prismatic geometries of C_s symmetries were tried for $MoCl_5$, and two slightly different configurations of this type could be fitted to the data. These geometries could conceptually be regarded as distorted C_{4v} square

pyramids; however, both of these models included some large vibrational amplitudes.[9] *Ab initio* calculations included in the present paper showed that these structures were about 15 kcal mol^{-1} higher in energy than the D_{3h} configuration, leaving the question of the geometry of $MoCl_5$ unresolved.

All this conflicting evidence has motivated us to undertake a reinvestigation of the structure of gas-phase $MoCl_5$. New GED data have been recorded and analyzed. Also previous *ab initio* calculations have been refined and extended in parallel with the experimental work. In this paper we present the results of these efforts.

Molecular orbital investigation

Calculations. *Ab initio* calculations for $MoCl_5$ were carried out along two different lines. In one series of computations an ordinary basis of Gaussian orbitals in Restricted Hartree–Fock (RHF) calculations was applied. The Cl basis is a (10,6,1) basis by Roos and Siegbahn[10] which is used in a segmented contraction to (6,4,1). The Mo basis is a (16,10,7) set developed by Fægri and Biran;[11] this set was used uncontracted. These calculations were carried out using the program DISCO.[12]

In the second series of calculations the same contracted

---

* To whom correspondence should be addressed.

Cl basis was utilized, but Mo was now described by a relativistic effective core potential (RECP). The RECPs developed by Hay and Wadt[13] were used with the extensions described by Petterson and coworkers.[14] The outer core orbitals 4s and 4p are included in the valence shell, permitting the use of this basis for correlated calculations. The basis sets for Mo are thus (6,5,5,3/5,4,4,1). Using the program system MOLECULE-SWEDEN,[15] both RHF and modified coupled pair functional (MCPF)[16] calculations were performed. The orbitals correlated in the MCPF calculations are mainly those that describe the Mo–Cl bonds, the open shell on Mo, and higher lying valence orbitals on Cl, for a total of 16 correlated orbitals.

All geometry optimizations have been carried out by calculating a sufficient number of grid points in the space spanned by the structural parameters, fitting a second degree polynomial to the data and interpolating for the minimum. Where necessary, values calculated for the interpolated minimum have been included in the grid for a further refinement till results were self-consistent.

Results and discussion. $MoCl_5$ has an odd number of electrons, and molecules of D_{3h} or C_{4v} symmetry would contain one electron in a doubly degenerate orbital, 6e″ or 16e, respectively. Thus both of these highly symmetric arrangements should be Jahn–Teller unstable.

The unconstrained optimization of the structure of $MoCl_5$ would require the variation of 12 structural parameters and be extremely costly. Partly on this background, and partly because of early experimental results which are interpreted in terms of a mixture of D_{3h} and C_{4v} structures, it was chosen first to explore the relative energies of $MoCl_5$ under the assumption of high symmetry. The results from these calculations are collected in Table 1, which shows all three computational approaches to yield results in very close agreement: the D_{3h} structure is energetically favoured by 10–11 kcal mol^{-1}.

Table 1. Optimized relative energies (ΔE) and structural parameters of D_{3h} and C_{4v} models of $MoCl_5$ obtained at three computational levels; all electron restricted Hartree–Fock (AE RHF) calculations; relativistic effective core (REC) RHF calculations; and RECP modified coupled pair functional (MCPF) calculations.

Parameter	Computational level		
	AE RHF	RECP RHF	RECP MCPF
D_{3h} Model[a]			
ΔE/kcal mol^{-1}	0	0	0
$r(Mo-Cl_a)$/pm	232.1	231.8	231.9
$r(Mo-Cl_e)$/pm	224.7	224.0	225.6
C_{4v} Model[b]			
ΔE/kcal mol	10.0	11.0	10.2
$r(Mo-Cl_{ap})$/pm	222.4	221.9	222.9
$r(Mo-Cl_{ba})$/pm	229.9	229.4	229.4
$\angle Cl_{ap}-Mo-Cl_{ba}$/°	100.4	101.3	100.9

[a] a = axial, e = equatorial. [b] ap = apical, ba = basal.

Table 2. Relative energies (ΔE) in kcal mol^{-1} of the two structures of C_s symmetry suggested in Ref. 9 obtained at three computational levels.

Model	Computational level		
	AE RHF	RECP RHF	RECP MCPF
$C_s(I)$	13.4	14.7	15.4
$C_s(II)$	15.5	15.1	15.8

The optimal D_{3h} structure has two axial ligands at a somewhat longer distance (6–8 pm) than the three equatorial Cl atoms. In the C_{4v} geometry crowding pushes the four basal Cl atoms further out than is the case for the D_{3h} structure, whereas the distance from Mo to the apical Cl is shorter than any of the other Mo–Cl distances. The inclusion of correlation through MCPF calculations yields no dramatic changes of any structural parameters, the most notable being a 1.6 pm lengthening of the equatorial Mo–Cl bond in the D_{3h} form.

Thus calculations for highly symmetric forms of $MoCl_5$ indicate that the trigonal bipyramidal form should be the most stable. This does not take into account the Jahn–Teller effect, which predicts that symmetry breaking should lower the energy. The Jahn–Teller effect does, however, not indicate the extent of this symmetry breaking. The latest GED results[9] of C_s symmetries were conceptually related to distortions of the C_{4v} form. In order to investigate the energy of these models relative to the C_{4v}, RHF and MCPF calculations were carried out for the two proposed models. In Table 2 it is shown that all the three computational approaches give energies for these C_s structures 3.4–5.6 kcal mol^{-1} higher than for the undistorted C_{4v} structure, and 13–16 kcal mol^{-1} above the D_{3h} configuration. Thus neither of these two C_s models appears to be a likely molecular structure of $MoCl_5$.

It therefore seems natural to take the lowest-energy

Table 3. Relative energies (ΔE) and structural parameters of the $^2B_1$ and the $^2A_2$ states of $MoCl_5$ optimized under the constraints of C_{2v} symmetry and obtained at the RECP SCF level, with the $^2E''$ state of a D_{3h} model included for comparison.

Parameter	Electronic state		
	$^2B_1$	$^2E''$	$^2A_2$
ΔE/kcal mol^{-1}	−0.24	0	−0.35
$r(Mo-Cl_{e1})$/pm[a]	225.0	224.0	221.3
$r(Mo-Cl_{e2})$/pm[a]	223.3	224.0	225.4
$r(Mo-Cl_a)$/pm[a]	231.9	231.8	231.6
$\angle Cl_a-Mo-Cl_a$/°	181.1[b]	180	172.4
$\angle Cl_{e2}-Mo-Cl_{e2}$/°	123.7	120	120.3

[a] The two Cl_a are the pseudo-axial atoms in the symmetry plane, Cl_{e1} is the pseudo equatorial atom in the symmetry plane, and the two Cl_{e2}s are mirror images in this plane. [b] $\angle Cl_a-Mo-Cl_{e1} = 89.4°$.

high-symmetry form, the D_{3h} form, for the starting point of Jahn–Teller distortions. Distortion to C_{2v} geometry would split the doubly degenerate 6e″ orbital into an a_2 and a b_1 orbital.[17] This distortion leaves five structural parameters to be optimized: the Mo–Cl$_a$, the Mo–Cl$_{e1}$ and the Mo–Cl$_{e2}$ bond distances and the valence angles $\angle$ Cl$_a$–Mo–Cl$_a$ and $\angle$ Cl$_{e2}$–Mo–Cl$_{e2}$. With this many parameters a grid of 21 points is required for fitting a second-degree polynomial; in practice more points than this are needed, as the grids for the $^2B_1$ and $^2A_2$ configurations do not coincide. For this reason it has only been possible to carry out RECP RHF calculations for the C_{2v} structures, but on the basis of the results of the high-symmetry forms we expect the structural influence of correlation to be rather small. Results for the two C_{2v} forms are presented in Table 3. The $^2A_2$ state is more stable than the $^2B_1$, but the energy differences are quite small, with the two Jahn–Teller distorted forms 0.24 and 0.35 kcal mol^{-1} below the D_{3h} form. The distortions from D_{3h} symmetry mainly take the form of changes in the pseudo-equatorial Mo–Cl bonds. For the $^2B_1$ form the Mo–Cl$_{e2}$ bonds are shortened, while the Mo–Cl$_{e1}$ bonds are elongated. For the $^2A_2$ form the changes are in the opposite direction. The shortening of the Mo–Cl$_{e2}$ bonds in the $^2B_1$ form is accompanied by a slight opening of the angle between them. No reduction of this bond angle is seen with the lengthening of these same bonds in the $^2A_2$ form, but the angle between the two pseudo axial bonds is reduced by 8°.

Mulliken population analysis carried out for the various forms shows large variations between the all-electron and the RECP RHF calculations; the former yield a charge of almost +1.7 on Mo, whereas the latter give +0.6. The reason is that the RECP Mo basis, with its greater valence and polarization space, particularly for the p-orbitals, is able to describe parts of the electron distribution which must be left to the Cl orbitals for the smaller all-electron basis. Some qualitative insight may still be obtained from the population analysis. The RECP results show a promotion of almost one electron from the 5s^{1}4d^5 configuration of 5p orbitals, indicating some degree of hybridization both for the D_{3h} and the C_{4v} forms. The electron distribution between s-, p- and d-orbitals on Mo is almost identical for both of these high-symmetry forms, and it is tempting to conclude that steric interactions rather than hybridization considerations determine the geometry of MoCl$_5$.

Gas electron-diffraction investigation

Experimental and data reduction. MoCl$_5$ with a stated purity >99.9% was purchased from Aldrich Chemie. GED data were recorded on Balzers Eldigraph KDG-2[18] with a brass inlet system and a nozzle temperature of 131 ± 5°C corresponding to a vapour pressure of 4 Torr.[19] Additional pertinent parameters for the experimental intensities are given in Table 4. Optical densities were recorded on the Snoopy densitometer and processed by

Table 4. Some parameters for the electron diffraction diagrams for MoCl$_5$ at about 42 keV.

Data set	1	2
Camera distance/mm	498.74	248.99
Wavelength/pm	5.873	5.873
Applied s-range/nm^{-1}	18.75–152.50	30.00–280.00
Increment Δs/nm^{-1}	1.25	2.50
No. of plates	6	6
Least-squares weights	1.0	0.2
R-factor (%)[a]	2.2	6.8

[a] Unweighted values for the average modified molecular intensities according to the deviations from the data of the single plates.

standard procedures;[20,21] atomic scattering factors from Ref. 22 were applied and backgrounds were drawn as fifth- and sixth-degree polynomials to the differences between experimental and the different calculated intensities for the long and short camera distance data, respectively. The average modified intensity points for the data from each camera distance are shown in Fig. 1.

Initial least-squares calculations. Least-squares calculations for four different symmetry point groups are summarized in Table 5. To characterize the accuracy of the different least-squares refinements given in Tables 5–7, a weighted percentage R factor according to eqn. (1) was

$$R = 100 \left(\frac{\sum \left[w(I_{obs} - I_{calc})^2 \right]}{\sum w I_{obs}^2} \right)^{1/2} \tag{1}$$

evaluated. All least-squares calculations were performed with a diagonal weight matrix. The least-squares standard deviations were therefore doubled to take care of the uncertainty due to data correlation.[23] Furthermore, an uncertainty in the scale of 0.1% was added to the
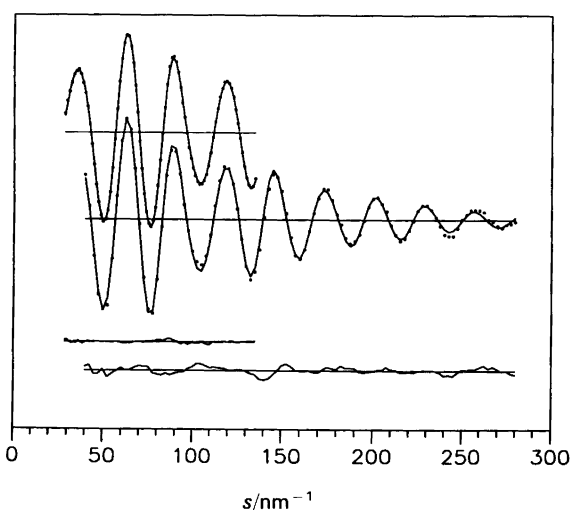

Fig. 1. Average experimental modified molecular intensities (dots) compared to the calculated ones for Refinement 2 of Table 6 (full line). The difference curve is given below.

Table 5. Refinements of various models of $MoCl_5$; the number of independent parameters refined relative to the total and the weighted R-factors for the best models are given.

Parameter	Molecular point group			
	D_{3h}	C_{4v}	C_s	C_{2v}
Independent bond distances	2/2	2/2	2/3	2/3
Independent valence angles	0/0	1/1	3/5	2/2
Mo–Cl vibrational amplitudes	2/2	1/2	1/3	2/3
Cl–Cl vibrational amplitudes	3/3	3/3	2/5	2/5
R-factor (%)	7.72	5.79	6.58	3.76

standard deviations of the distance parameters. All standard deviations in Tables 6 and 7 were corrected in this way.

The refinements of Table 5 all result in larger Cl–Cl vibrational amplitudes than one would expect for rigid molecules. Thus, in agreement with the earlier results[5] neither a rigid D_{3h} nor a rigid C_{4v} molecule fits the present data sufficiently accurately; neither do the C_s models proposed in Ref. 9 with respect to the new data. Only C_{2v} models were found to give an adequate agreement with the present data.

Refinements based on the C_{2v} model. The initial refinements and the first refinements based on a C_{2v} symmetry model were performed before the *ab initio* results of Table 3 were available. The C_{2v} model is described by three bond distances and two valence angles, and contains five different nonbonded Cl···Cl distances. Exploratory refinements indicated that the best model was closer to D_{3h} than to C_{4v} symmetry. The results of two different refinement schemes with $\angle Cl_a$–Mo–Cl_a and $\angle Cl_{e2}$–Mo–Cl_{e2} as the two independent valence angles are given in Table 6. In Refinement 1 the three pseudo-
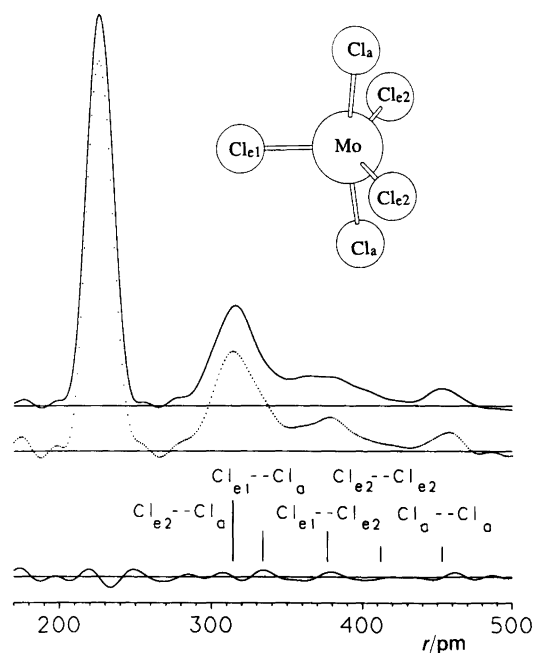

Fig. 2. Experimental (lower) and calculated (upper) radial distribution functions for an artificial damping constant of 25 pm^2 with differences given below. The calculated function is based on the parameters in Refinement 2 of Table 6 for a C_{2v} symmetric model. The notation of the atoms in the molecule are shown and the positions of the five nonbonded Cl···Cl distances are indicated.

equatorial bonds were assumed to be equal, while their difference in Refinement 2 was fixed at the *ab initio* difference of the $^2A_2$ form of 4.1 pm. In addition, the refinement scheme for the vibrational amplitudes differs in the two refinements. In Refinement 1 the amplitude of the Mo–Cl_a distance is especially large for a bonded distance. All the amplitudes of the nonbonded distances of Refine-

Table 6. Internuclear distances (r_a), root mean-square vibrational amplitudes (l) and valence angles of $MoCl_5$ of C_{2v} symmetry obtained by least-squares refinements on the gas electron diffraction data, with estimated standard deviations in units of the last digit given in parentheses.

	Refinement 1		Refinement 2	
	r_a/pm	l/pm	r_a/pm	l/pm
Mo–Cl_{e1}[a]	225.4(3)[1,b]	6.1(7)[2]	222.1(5)[5]	6.7(3)[6]
Mo–Cl_{e2}	225.4(3)[1]	6.1(7)[2]	226.3(5)[5]	6.7(3)[6]
Mo–Cl_a	227.1(5)	8.1(10)	227.8(7)	6.7(3)[6]
Cl_{e2}···Cl_a	313.0(3)	11.8(5)[3]	314.2(8)	12.4(4)
Cl_{e1}···Cl_a	336.9(7)	15.8(7)[3]	334.0(14)	23.2(34)
Cl_{e1}···Cl_{e2}	377.7(7)	14.9(7)[4]	376.8(13)	19.9(25)[7]
Cl_{e2}···Cl_{e2}	412.6(13)	14.9(7)[4]	412.2(22)	19.9(25)[7]
Cl_a···Cl_a	451.7(9)	9.0(10)	453.2(13)	10.3(26)
$\angle Cl_a$–Mo–Cl_a/°	167.6(2)		168.2(5)	
$\angle Cl_{e2}$–Mo–Cl_{e2}/°	132.4(6)		131.2(12)	
$\angle Cl_{e1}$–Mo–Cl_{e2}/°	113.8(7)		114.4(13)	
R-factor (%)	3.76		3.62	

[a] For the labeling of the Cl atoms see footnote to Table 3 or Fig. 2. [b] Parameters with the same superscripted number were refined with a constant difference.

Table 7. Geometrical parameters of and least-squares results for a simple dynamical model for $MoCl_5$ based on the *ab initio* results. Only the three parameters with given standard deviations could be varied in the least-squares calculation.

Parameter and description	*Ab initio* values	Least-squares values
g_1, scale factor[a]	1.000	0.9957(30)
g_2/pm, barrier position[b]	224.0	224.0
g_3/kcal mol^{-1}, ΔE of $^2B_1$	−0.24	−0.24
$g_4/°$, $\angle Cl_a$–Mo–Cl_a of $^2B_1$	181.1	181.1
$g_5/°$, $\angle Cl_{e2}$–Mo–Cl_{e2} of $^2B_1$	123.7	123.7
g_6/kcal mol^{-1}, ΔE of $^2A_2$	−0.35	−0.35
$g_7/°$, $\angle Cl_a$–Mo–Cl_a of $^2A_2$	172.4	155.2(9)
$g_8/°$, $\angle Cl_{e2}$–Mo–Cl_{e2} of $^2A_2$	120.3	135.0(16)
R-factor (%)		5.66

[a] Scale factor between the *ab initio* and the electron diffraction distances. [b] Position of the potential barrier ($\Delta E = 0$ kcal mol^{-1}) along r_{e1}, the chosen independent parameter of the potential.

ment 2 are larger than the ones obtained in Refinement 1. Generally the vibrational amplitudes obtained in these least-squares refinements are greater than the amplitudes computed from spectroscopic data for a rigid D_{3h} molecule.[5] According to these refinements free $MoCl_5$ exhibits some large–amplitude motion, the average over this motion fits slightly different C_{2v} structures very well. The modified molecular intensities calculated for Refinement 2 are matched to the experimental ones in Fig. 1, and the corresponding radial distribution functions are compared in Fig. 2.

Refinements based on the ab initio *result.* According to the *ab initio* result of Table 3, a large-amplitude motion of $MoCl_5$ may be described as some weighted average of a motion from the $^2B_1$ state to the $^2A_2$ state. Firstly an attempt was made to refine the fraction of each of the two states in a mixture. Refinements of this type removed the $^2B_1$ species, and refinements on only the $^2A_2$ state ended in results corresponding to the results of Table 6.

A simple dynamical model based on the *ab initio* result was constructed in terms of the eight independent structural parameters given in Table 7. In this model, the molecule moves in two 2–4 potentials with minima at the two estimated C_{2v} geometries. The independent variable for these potentials was chosen to be the Mo–Cl_{e1} distance, since this distance was the parameter that varied over the largest range according to the *ab initio* calculations. The two potentials joined smoothly at a barrier in between the two forms placed at g_2. The Mo–Cl_{e2} and the $MoCl_a$ distances were assumed to vary linearly with the Mo–Cl_{e1} distance. Noting that the Mo–Cl_{e1} and the $MoCl_{e2}$ distances intersect very close to the *ab initio* value of the equatorial distance of the $^2E''$ state of D_{3h} symmetry, it seemed reasonable to assume that the molecule passes close to this geometry on its motion between the two minima. Accordingly, the barrier of the potential, g_2, was fixed on this value and the angle parameters were forced to pass through the trigonal bipyramid at this point. All the *ab initio* distances were scaled by the factor g_1, while the angles of the two forms were treated as the independent parameters g_4, g_5, g_7 and g_8. Nine

molecules with vibrational amplitudes computed from spectroscopic data for a D_{3h} symmetric $MoCl_5^5$ were placed in the potential at equidistant values of the Mo–Cl_{e1} distance with properly normalized Boltzmann weights. The potentials were assumed to raise steeply half an interval to the left of the $^2B_1$ and to the right of the $^2A_2$ minimum geometries (Fig. 3).
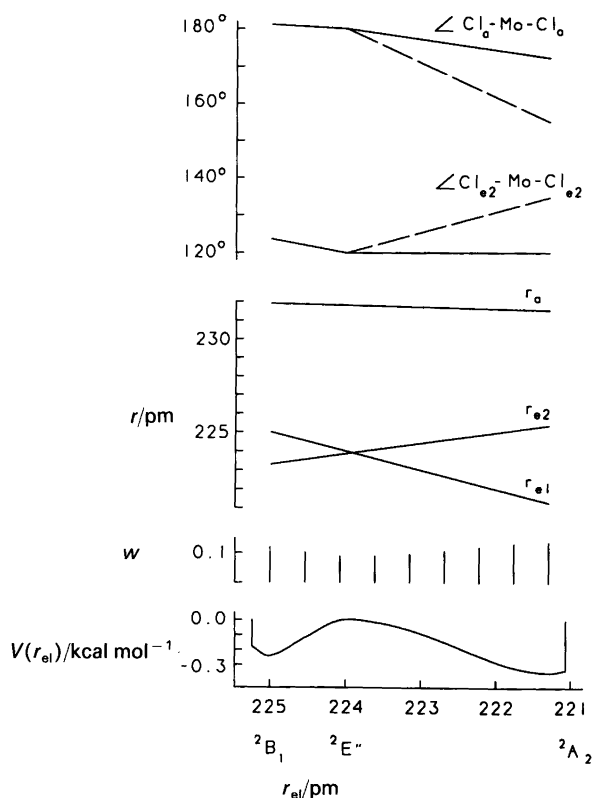

Fig. 3. The simple dynamical model of $MoCl_5$ based on the *ab initio* results. From below the applied potential, $V(r_{e1})$, the position of the nine rigid molecules and the sizes of their normalized Boltzmann weights (*w*), and the assumed variations of the geometrical parameters in the potential. The scale is the *ab initio* scale ($g_1 = 1$), and the variations of the angles according to the least-square values of Table 7 are given as broken lines. All quantities are given as functions of the chosen independent variable r_{e1}.

Refinement of only the scale factor, g_1, gave the value 0.9957(30), indicating that the electron-diffraction distances r_a in terms of this model are shorter than the *ab initio* distances by 0.4%. As Fig. 4 shows, this result does not agree very well with the experiment.

Refinements of g_4 and g_5, the angles of the $^2B_1$ state, lead to unreasonable values. Actually, removing this state from the model by fixing g_3 on a high positive value leads to almost no changes in the calculated radial distribution functions. The reason may be that going from the C_{2v} minimum of the $^2B_1$ state to the D_{3h} geometry, the molecule passes through approximately the same distance spectrum as the spectrum covered by the beginning of the range from the D_{3h} to the minimum for the $^2A_2$. Decreasing the relative amount of the former will increase the relative amounts of the latter state. This offers a possible explanation why the refinements on a mixture of the two states mentioned above led to removal of the $^2B_1$ configuration. Refinement of g_3, the relative energy of the $^2B_1$ state, breaks down. Neither would the relative energy of the $^2A_2$ state, g_6, refine.

The angles of the $^2A_2$ minimum geometry, g_7 and g_8, converged to 155 and 135°, respectively, indicating a greater deformation away from the D_{3h} geometry than the result of the *ab initio* calculation. These angles also correspond to a slightly greater deformation than was obtained for the C_{2v} structures of Table 6. Thus, this simple dynamic model, based on the *ab initio* result and additional more or less reasonable assumptions, allows
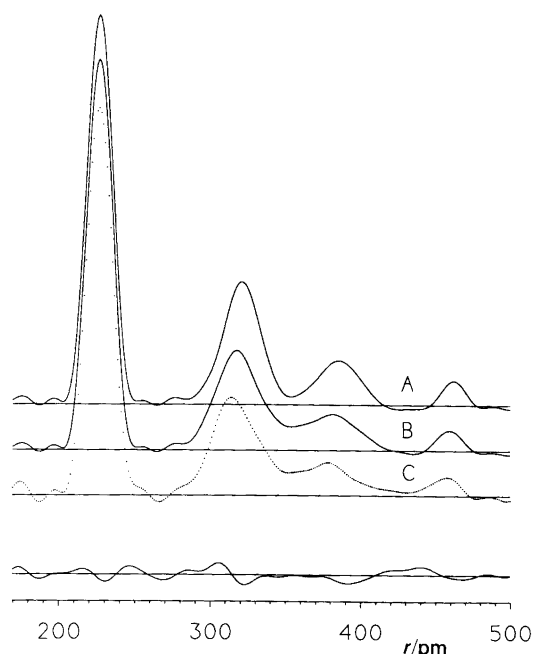

Fig. 4. Radial distribution functions based on the simple dynamical model for an artificial damping function of 25 pm². (A) Calculated function of the *ab initio* results only scaled to the GED data with $g_1 = 0.9957$. (B) Function computed according to the least-squares values of Table 7. (C) Experimental curve. The differences between C and B are given.

the refinement of three geometrical parameters. This refinement ends on an R-factor of 5.7% and agrees surprisingly well with the experimental GED data, as Fig. 4 shows.

Conclusions

The *ab initio* results of Table 3 indicate that the degenerate $^2E''$ state of a free D_{3h} symmetric $MoCl_5$ molecule splits into two distorted states of C_{2v} symmetry, a $^2B_1$ and a $^2A_2$ state. The three states are within an energy range of 0.35 kcal mol^{-1}, and accordingly the molecule may be expected to undergo a dynamic Jahn–Teller distortion.

C_{2v} models exhibiting large-amplitude motions fit the electron-diffraction data very well (Table 6) and significantly better than models based on the other molecular point groups that have been tested (Table 5). This C_{2v} geometry corresponds to the *ab initio* geometry of the $^2A_2$ state. Even with the split of the two types of equatorial distances fixed on the *ab initio* split of the $^2A_2$ state, the obtained GED distances disagree with the *ab initio* distances by two to three times the estimated standard deviations, and the angular deformation of this C_{2v} model is larger than one would expect from the *ab initio* calculations.

A simple dynamic model for the GED data based on the *ab initio* results indicates that the GED data are very insensitive to a possible presence of the $^2B_1$ state, and that the electron-diffraction r_a distances are shorter than the *ab initio* values by a scale factor of 0.9957(30). The uncorrected least-squares standard deviation of this factor is 0.0002, and in addition computer simulations demonstrate that in relation to the GED data and in terms of this model, the factor is significantly smaller than one; however, this significance disappears when the uncertainty of the GED r-scale is included in the standard deviation. The angular deformations obtained for the $^2A_2$ state are larger than suggested by the *ab initio* results. Nevertheless, the $^2A_2$ state hits the potential wall well before the C_{4v} configuration is reached, and the molecule is not pseudorotating by the Berry mechanism.[24] This agrees with the *ab initio* result, which places the C_{4v} energy about 11 kcal mol^{-1} above the D_{3h} species.

Thus the results of the *ab initio* calculations and the electron-diffraction investigation agree if a relatively flat potential is assumed for the distortion from D_{3h} symmetry to the C_{2v} minimum of the $^2A_2$ state. This type of potential would reduce the accuracy of the GED estimates of the valence angles of the $^2A_2$ state, as well as making an accurate determination of these angles from *ab initio* methods very difficult.

The $MoCl_5$ related compound CrF_5 has been investigated by GED.[25] For this molecule a distortion from D_{3h} to C_{2v} geometry in the direction of the *ab initio* distortion of the $^2A_2$ state of $MoCl_5$ was observed. The angles $\angle F_a$–Cr–F_a and $\angle F_{e2}$–Cr–F_{e2} were determined as 168 and 128°, respectively. Thus according to the GED

data CrF_5 is somewhat less distorted than $MoCl_5$, and the vibrational amplitudes determined for CrF_5 indicate that this molecule is more rigid than $MoCl_5$. In view of the insensitivity of the GED data to the presence of a possible $^2B_1$ state according to the dynamical model, the main difference between the two molecules may be a flatter distortion potential for $MoCl_5$, and it is possible that both of the molecules exhibit the dynamical Jahn–Teller effect as predicted by the *ab initio* calculations of $MoCl_5$. However, in neither case is this conclusively confirmed by the GED investigations.

References

1. Sands, D. E. and Zalkin, A. *Acta Crystallogr. 12* (1959) 723.
2. Preiss, H. *Anorg. Allg. Chem. 389* (1972) 280.
3. Spiridonov, V. P. and Romanov, V. G. *Vestn. Mosk. Univ. Ser. II 22* (1967) 98.
4. Ezhov, Y. A. and Sarkin, A. P. *Zh. Struct. Khim. 24* (1983) 57.
5. Brunvoll, J., Ischenko, A. A., Spiridonov, V. P. and Strand, T. G. *Acta Chem. Scand., Ser. A 38* (1984) 115.
6. Beattie, I. R. and Ozin, G. A. *J. Chem. Soc. A.* (1969) 1691.
7. Bridson, A. K., Graham, J. T., Hope, E. G., Jenkins, D. M., Levason, W. and Ogden, J. S. *J. Chem. Soc., Dalton Trans.* (1990) 1529.
8. Haaland, A., Hammel, K., Rypdal, K. and Volden, H. V. *J. Am. Chem. Soc. 112* (1990) 4547.
9. Brunvoll, J., Gundersen, S., Ischenko, A. A., Spiridonov, V. P. and Strand, T. G. *Acta Chem. Scand. 45* (1991) 111.
10. Roos, B. and Siegbahn, P. *Theor. Chim. Acta 17* (1970) 199 and 209.
11. Fægri, K. and Biran, G. *J. Comput. Chem. 10* (1989) 495.
12. Almlöf, J., Fægri, K. and Korsell, K. *J. Comput. Chem. 3* (1982) 385.
13. Hay, P. J. and Wadt, W. R. *J. Chem. Phys. 82* (1985) 299.
14. Petterson, L. G., Bauschlicher Jr., C. W., Langhoff, S. R. and Partridge, H. *J. Chem. Phys. 87* (1987) 481.
15. MOLECULE-SWEDEN is an electronic structure program written by J. Almlöf, C. W. Bauschlicher, M. R. A. Blomberg, D. P. Chong, A. Heiberg, S. R. Langhoff, P.-Å. Malmquist, A. P. Rendell, B. O. Roos, P. E. M. Siegbahn and R. P. Taylor.
16. Chong, D. P. and Langhoff, S. R. *J. Chem. Phys. 84* (1986) 5606.
17. Bader, R. F. and Westland, A. *Can. J. Chem. 39* (1961) 2306.
18. Bastiansen, O., Graber, R. and Wegmann, L. *Balzers High Vacuum Rep. 25* (1969) 1.
19. Calculated from the Clausius–Clapeyron equation and thermodynamic quantities from Canterford, J. H. and Colton R. *Halides of Second and Third Row Transition Metals*, Wiley, New York 1968, p. 230.
20. Andersen, B., Seip, H. M., Strand, T. G. and Stølevik, R. *Acta Chem. Scand. 23* (1969) 3224.
21. Gundersen, S., Strand, T. G. and Volden, H. V. *J. Appl. Crystallogr. 25* (1992) 409.
22. Ross, A. W., Fink, M. and Hilderbrandt, R. *International Tables for Crystallography*, Kluwer Academic Publishers, Dordrecht 1992, Vol. C, p. 245.
23. Seip, H. M., Strand, T. G. and Stølevik, R. *Chem. Phys. Lett. 3* (1969) 617.
24. Berry, R. S. *J. Chem. Phys. 32* (1960) 933.
25. Jacob, J., Hedberg, L., Hedberg, K., Davis, H. and Gard, G. L. *J. Phys. Chem. 88* (1984) 1935.